

Communication pubs.acs.org/JACS

Catalytic Hydrogenolysis of Aryl C-F Bonds Using a Bimetallic Rhodium-Indium Complex

James T. Moore and Connie C. Lu*



Cite This: J. Am. Chem. Soc. 2020, 142, 11641-11646



ACCESS I

III Metrics & More

Article Recommendations

Supporting Information

ABSTRACT: A homogeneous rhodium-indium catalyst hydrodefluorinates substrates bearing strong aryl C-F bonds, including difluoro- and fluorobenzene, using 1 atm of H₂, alkoxide bases, and moderate temperatures (70-90 °C). Characterization of catalytic intermediates establishes a formal Rh^{-1}/Rh^{I} redox cycle. The $Rh \rightarrow In$ interaction is proposed to enable catalysis by stabilizing the reactive Rh⁻¹ species, which is responsible for cleaving the Ar-F bond and is ultimately regenerated using H₂ and

rganofluorines are an important class of industrial chemicals, accounting for 30% of agrochemicals and 10% of pharmaceuticals. However, their environmental persistence and toxicity to human health motivate efforts to develop processes that efficiently degrade organofluorines.²⁻⁵ Catalytic hydrodefluorination using H2 is a promising remediation strategy from the standpoints of sustainability and atom economy. An inherent challenge in hydrodefluorination is overcoming the chemical inertness of the C-F σ bond (~500 kJ/mol).6 While only a few transition metal catalysts can activate alkyl C-F bonds, 7-10 metal-mediated aromatic C-F bond cleavage is better established. However, most of these catalysts react only with highly fluorinated substrates, 11-18 where the C-F bonds are considerably weaker than those present in arenes bearing fewer F atoms, e.g. C₆H₅F and $C_6H_4F_2$. 19-23 From the metal viewpoint, one issue is that relatively strong M-F bonds are formed.²³⁻²⁹ Hence, most catalysts require strongly fluorophilic reductants to drive fluoride elimination. ^{13,14,18} For example, the Nb catalyst shown in Figure 1 hydrodefluorinates fluorobenzene, but requires H₃SiR to abstract fluoride from Nb.²² Lastly, the lack

Rh/Al₂O₃ Dipp -NMe₂ this work

Figure 1. Selected catalysts for the hydrodefluorination of fluorobenzene. 9,22,3

of selectivity in activating C-F bonds over C-H bonds in partially fluorinated arenes can be problematic.^{26,27}

For the hydrogenolysis of aryl C-F bonds, the state-of-theart catalyst is a heterogeneous Rh/Al₂O₃ system, which converts fluorobenzene to cyclohexane quantitatively at ambient temperature and 1 atm of H_2 . Among molecular catalysts, the bimetallic Ru/Pd complex is the most active (Figure 1).9 The Ru/Pd catalyst hydrodefluorinates fluorobenzene to benzene quantitatively using NaOt-Bu in i-PrOH at 80 °C. The Pd site is proposed to activate the C-F bond³² while the Ru center mediates the transfer-hydrogenation reaction.³³ In both of these systems, mechanistic understanding is lacking with only scant experimental data for any metal-based intermediates.

Here, we describe the hydrodefluorination of aryl C-F bonds using a bimetallic Rh-In catalyst with 1 atm of H2 and NaOt-Bu as the stoichiometric base. A catalytic cycle is proposed where an anionic Rh-In active species performs oxidative cleavage of the aryl C-F bond, releasing F-. The resulting Rh-In aryl intermediate then reacts with H2, forming the hydrodefluorinated arene and a Rh-In hydride. The latter regenerates the anionic active species after sequential H₂ binding, deprotonation, and H₂ release. Several of the proposed intermediates have been isolated and structurally characterized, and their stoichiometric reactivity profiles support the proposed mechanism.

The synthesis of the Rh-In catalyst began with the installation of Rh(I) into the metalloligand, $In[N(\emph{o} (NCH_2Pi-Pr_2)C_6H_4)_3$ ³⁴ (abbrev. InL), using 0.5 equiv of $\{Rh(\mu-Cl)(C_2H_4)_2\}_2$, affording Cl-RhInL (1). Metathesis of the Cl ligand with NaHBEt₃ at -78 °C provided the hydride,

Received: May 5, 2020 Published: June 18, 2020





H–RhInL (2). Both 1 and 2 are Rh(I) → In(III) complexes (Figures S2–S6), where the In ion acts as a σ -acceptor Z-type ligand. These synthetic preparations are analogous to those reported for the isostructural Rh–Al and Rh–Ga complexes, and are reminiscent of other Rh–group 13 systems. The deprotonation of 2 using n-BuLi at −78 °C under N₂ afforded the rhodate complex, Li(THF)_x[(N₂)-RhInL], 3-N₂ (Figures S13–S14). The N₂ ligand is labile ($\nu_{\rm N-N}=2095~{\rm cm}^{-1}$, KBr pellet, Figure S17), and exposure of 3-N₂ to vacuum or Ar formed the "naked" Li(THF)_x[RhInL] (3) with a color change from yellow to dark green. Under 1 atm of H₂, 3-N₂ converted to the H₂ adduct, Li(THF)_x[(η^2 -H₂)RhInL] (3-H₂), which displayed a characteristic ¹H{³¹P} NMR doublet at −5.10 ppm ($J_{\rm Rh-H}=18.2~{\rm Hz}$, 2H).

The solid-state structures of 2 and 3-N₂ are shown in Figure 2. Complex 2 features a 5-coordinate Rh center that is

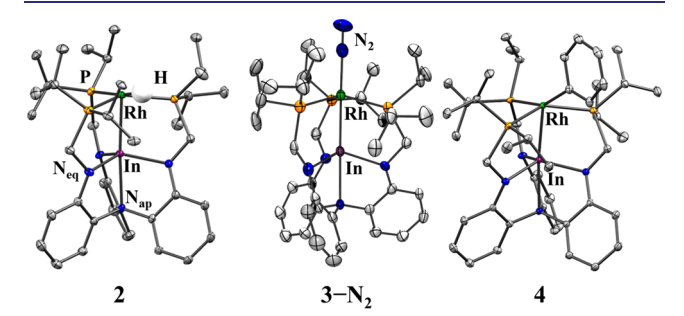


Figure 2. Solid-state structures of H–RhInL, (2), $\text{Li}(\text{DME})_3[(N_2)-\text{RhInL}]$, (3–N₂), and Ph–RhInL, (4) shown at 50% probability level. See Supporting Information for the structure of 1 and additional details.

approximately square pyramidal. The phosphines are coplanar with the hydride, which was located in the Fourier difference map. In 3-N₂, the Rh center is trigonal bipyramidal, where the axial N₂ ligand is positioned *trans* to In. During an attempted crystallization of 3-N₂ from a THF/PhF solvent mixture, dark-red crystals were formed, whose identity was established by X-ray diffraction to be Ph–RhInL (4). Complex 4 (Figure 2) has a 5-coordinate Rh center that is distorted between square pyramidal and trigonal bipyramidal geometries. Across the three structures, the Rh–In bond length is almost invariant

(2.54 to 2.56 Å, Tables S1–S3), and is substantially smaller than the sum of the metals' covalent radii (2.84 Å),⁴⁵ lending support for a strong Rh \rightarrow In interaction.

The serendipitous formation of 4 from the reaction of $3\text{-}N_2$ and PhF inspired us to investigate $3\text{-}N_2$ as a hydrodefluorination catalyst. Previously, $(C_5\text{Me}_5)\text{Rh}(\text{PMe}_3)\text{H}_2$ was reported to react with highly fluorinated arenes in a benzene/pyridine solvent mixture at 85 °C to afford $(C_5\text{Me}_5)\text{Rh}(\text{aryl}^F)$ -H. The authors proposed that the anion, $[(C_5\text{Me}_5)\text{Rh}(\text{PMe}_3)\text{H}]^-$, was the active species that cleaves the aryl C–F bond. Attempts to catalyze the hydrodefluorination of C_6F_6 using H₂, however, were not promising. Other Rh complexes were later demonstrated to perform catalytic hydrogenolysis of aryl C–F bonds with stoichiometric bases. Tr,31,48,49 However, these catalysts were only able to activate highly fluorinated arenes or 1-fluoronaphthalene, and were unreactive with PhF.

To optimize the catalytic conditions, o-difluorobenzene (o-DFB) was selected as the test substrate (Table 1). At 15 mol % catalyst loading, 2.5 equiv of LiOt-Bu, 1 atm of H₂, and 70 °C in THF, both Rh-Cl 1 and Rh-H 2 were equally effective at yielding PhF quantitatively within 24 h (entries 1-2). By prolonging the reaction time to 48 h, both 1 and 2 gave further defluorination of PhF to benzene, albeit in low yields of 24% and 11%, respectively. Raising the H₂ pressure to 2 and 4 atm for 1 decreased the yield of PhF to 96% and 30%, respectively (entries 3-4). Entries 5 and 6 illustrate that, for 1 with LiOt-Bu, both lower (50 °C) and higher (90 °C) temperatures resulted in lower PhF yields of 87% and 63%, respectively. Next, decreasing the catalyst loading to 5 mol % 1 (entry 7) increased PhF turnovers to ~17 while maintaining a good yield of 87% at 48 h. When LiOt-Bu was increased to 10 equiv at 5 mol % 1 (entry 8), the yield fell slightly to 78% at 48 h. Changing the base to NaOt-Bu (2.5 equiv), which should be a stronger base due to weaker ion pairing, 50 and using 3 mol % 1 gave the highest turnovers of PhF (~30) while maintaining a high total yield of 93%. As a control, no baseline reactivity was found in the absence of catalyst (entry 10).

The Rh–Al and Rh–Ga chloride complexes also showed limited activity but performed worse than 1 (entries 11-12). The poor activity of the lighter group 13 congeners likely stems from the Rh electronics, which depends on the group 13 identity. Specifically, the Rh(-I/0) redox potentials for the

Table 1. Catalytic Hydrodefluorination of o-DFB Under Various Conditions^a

	•	•						
entry	precatalyst	Catalyst loading (mol %)	H ₂ Pressure (atm)	Temp (°C)	PhF equiv, $t = 24 \text{ h}$	PhF turnovers, $t = 48 \text{ h}$	PhH equiv, $t = 48 \text{ h}$	% total yield, $t = 48 \text{ h}$
1	1	15	1	70	6.67(1)	6.67(1)	1.6(1)	quantitative
2	2	15	1	70	6.67(1)	6.67(1)	0.76(7)	quantitative
3	1	15	2	70	5.62(4)	6.37(6)	trace	96
4	1	15	4	70	1.3(7)	1.99(5)	0	30
5	1	15	1	50	4.0(2)	5.8(4)	0	87
6	1	15	1	90	2.80(9)	4.2(7)	0	63
7	1	5	1	70	12.3(2)	17.3(3)	0.14(7)	87
8 ^d	1	5	1	70	11.3(1)	15.6(9)	trace	78
9 ^e	1	3	1	70	14(3)	31(2)	3(2)	93
10	none	n/a	1	70	0	0	0	0
11	Cl-RhAlL	15	1	70	0.09(4)	0.3(1)	0	4
12	Cl-RhGaL	15	1	70	1.4(3)	2.7(5)	trace	40

^aInitial catalytic conditions unless otherwise noted: precatalyst (15 mol %), 1 atm of H₂, 2.5 equiv of LiOt-Bu in THF at 70 °C. Triplicate runs. ^bPhF turnovers also count any PhF further converted to PhH. ^cCombined yield of PhF, PhH. Maximum yield based on o-DFB. ^d10 equiv of LiOt-Bu. ^e2.5 equiv of NaOt-Bu.

[RhML] series increase as M is varied down group 13 (V, vs $FeCp_2^{+/0}$, Figures S20-S21): -1.61 (M = Al) < -1.51 (Ga) < -1.35 (In). The more reducing rhodate species, [RhAlL] and [RhGaL] (X-ray, Figure S19), are likely more difficult to form during catalysis than the corresponding Rh-In counterpart, making turnover sluggish.

Next, the substrate scope of catalyst 1 was probed with various fluoroarenes, using standard conditions from the o-DFB optimization shown in Figure 3. The substrate p-F-

Figure 3. Substrate scope for catalyst 1 using standard conditions unless otherwise specified (Table S4, Figures S22-S35). The reactive halogen atoms are highlighted in yellow. "Standard catalytic conditions unless otherwise specified. bAvg of triplicate trials. c1.25 equiv of NaOt-Bu. ^d6-8 mol % cat. ^e1.8 mol % cat. ^f90 °C.

(CF₃)C₆H₄ was converted cleanly to PhCF₃ (99% yield), demonstrating that alkyl C-F bonds are unreactive. The substrate 2,5-F₂-toluene was monodefluorinated to o-F-toluene in moderate yield, suggesting that sterics can dictate selectivity. Next, reactions with the p-dihaloarenes p-F-XC₆H₄, where X is Cl or I, showed the preference for cleaving the weaker C-X bond over the C-F one. We note that this reactivity profile contrasts with traditional S_NAr and is more in line with the periodic trends observed in oxidative addition. 51-53 Small amounts of the PhF product (3 to 9%) further reacted to form

Unlike o-DFB, both p- and m-DFB did not convert significantly under standard conditions.²² Hence, these reactions were heated to 90 °C for ~3 days. The hydrogenolysis of p-DFB produced mostly PhF (65% yield) and some C₆H₆ (9%). The hydrogenolysis of m-DFB gave more C₆H₆ than PhF (3:2 ratio), though this difference may be attributed to the higher catalyst loading (7.5 mol %) used for m-DFB. Excitingly, 1 (7.5 mol %) hydrodefluorinated PhF to C₆H₆ with nearly full conversion (98% yield) after heating at 90 °C for ~5 days (Figures S28-S29, S36).

The complementary strategies between fluorination and deuteration to enhance the metabolic lifetime of pharmaceuticals prompted us to investigate the efficacy of 1 for catalytic deuterodefluorination. 32,53 Under 1 atm of D2 and otherwise standard conditions, 1 transformed both o-DFB and p-F-(CF₃)C₆H₄ into the expected monodeuterated arene as the

major product (≥70% yield, Figures 4, S37-S44). For the reaction with o-DFB, the ¹H NMR integrations appeared

Figure 4. (a, b) Deuterodefluorination of o-DFB and p-fluorobenzotrifluoride under standard catalytic conditions. Only major product/ isomer is shown. Proton NMR integrations reflect the overall mixture. (c) Stochiometric reaction of 4 with excess HBpin.

consistent with the incorporation of 1 equiv of D at the ortho position (Figure 4a). However, in the ¹⁹F NMR spectrum (Figure S40), three unique resonances were resolved, corresponding to PhF- d_1 (76%), PhF (14%), and PhF- d_2 (10%). The formation of PhF- d_2 supports the co-occurrence of aryl C-H bond activation, which should result in the production of HD from C-H/C-D scrambling. Hydrodefluorination with the generated HD could lead to PhF, although the larger yield of PhF versus PhF-d2 points to other unknown protio-sources. The substrate p-F-(CF₃)C₆H₄ was also defluorinated to form trifluorotoluene- d_1 , with $\sim 70\%$ deuterium incorporation at the para position (Figure 4b). Approximately ~20% of the deuterium was incorporated into the meta position, which suggests that aryl C-H bond activation occurs ortho to C-F bonds. 54,55 This regioselectivity shows that C-H activation is dictated by pK_a , which is lowered dramatically with an ortho fluorine. 19,27 Collectively, these results show that reversible C-H activation, while competitive, does not impede C-F activation.

Scheme 1 illustrates the proposed catalytic cycle for the hydrodefluorination of PhF to benzene. Starting from 1, addition of H2 and tert-butoxide initiates the catalytic cycle by forming the hydride 2 (Figures S45-S46). Reversible binding of H₂ provides the Rh(I) hydride/H₂-adduct, 2-H₂. Deprotonation of the bound H2 by tert-butoxide forms a transient Rh(I) dihydride, which relaxes to the Rh(-I) H_2 -adduct, 3- H_2 . So Reversible loss of H_2 generates the unsaturated Rh(-I)active species 3, which oxidatively cleaves the C-F bond, producing NaF and the Rh(I) phenyl complex, 4. In the last step, 4 reacts with H₂ to produce benzene and 2, which reenters the catalytic cycle.

Consistent with this mechanism, the Rh(I) hydride 2 under H₂ formed a new species, as suggested by the appearance of a broad ¹H NMR peak at -4.83 ppm (Figures S7-S12). This peak decoalesced at -80 °C into two peaks at -5.10 and -9.85 ppm, consistent with the H_2 and H ligands, respectively, of 2-H₂. Additionally, the $T_{1(min)}$ values of 30.9 and 35.8 ms

Scheme 1. Proposed Cycle for Hydrogenolysis of Fluorobenzene by the Rh-In Catalyst

(400 MHz) are characteristic of intact H₂ ligands in complexes 2-H₂ and 3-H₂, respectively (Figures S50-S51).⁵⁷⁻⁵⁹ From a reactivity standpoint, 2 cannot be deprotonated with tertbutoxide on its own; but when H2 is present, 2-H2 can be converted to $3-H_2$. The conversion of 3 in PhF/C₆H₆ to 4, described above, supports the proposed C-F bond activation by the unsaturated rhodate(-I) center in 3. Additionally, ¹⁹F NMR analysis of the nonvolatiles from a catalytic run revealed the presence of NaF (Figure S49).⁶⁰ A sample of isolated 4 reacted rapidly with H₂ (1 atm) in THF to yield benzene and 2 (Figures \$47-\$48). During catalysis, the catalyst resting state depended on the identity of the base: 3-H2 was observed for NaOt-Bu, and 2-H₂, for LiOt-Bu (Figures S45-S46). These rate-limiting steps, deprotonation of 2-H₂ and its subsequent H_2 loss, both precede formation of the unsaturated Rh(-I)active species. As an aside, 4 also reacted with HBpin to afford 2 and PhBpin, completing a synthetic cycle for the borylation of PhF using HBpin (Figures 4c and S52-S54).61-68 Unfortunately, no turnover was observed for HBpin and o-DFB.

In closing, we report a new catalyst for hydrodefluorination of unactivated aryl C–F bonds using H₂ as the reductant, rather than silanes or boranes. Notably, each step in the catalytic cycle was studied through either isolation or *in situ* characterization of intermediates. Collectively, these results show that leveraging direct Lewis acid–transition metal interactions is a viable strategy for the activation of strong C–F bonds under mild conditions. Future efforts seek to expand the substrate scope and to render the C–F borylation of aryl fluorides catalytic.

ASSOCIATED CONTENT

Supporting Information

The Supporting Information is available free of charge at https://pubs.acs.org/doi/10.1021/jacs.0c04937.

Experimental procedures, characterization and spectroscopic data (PDF)

X-ray crystallographic data for complexes 1, 2, 3-N₂, 4, $K(THF)_3$ -RhAlL, and $Li(DME)_2[RhGaL]$ have been deposited in the Cambridge CCDC as numbers 2009345–2009350 (CIF)

AUTHOR INFORMATION

Corresponding Author

Connie C. Lu — Department of Chemistry, University of Minnesota, Minneapolis, Minnesota 55455-0431, United States; orcid.org/0000-0002-5162-9250; Email: clu@umn.edu

Author

James T. Moore – Department of Chemistry, University of Minnesota, Minneapolis, Minnesota 55455-0431, United States

Complete contact information is available at: https://pubs.acs.org/10.1021/jacs.0c04937

Notes

The authors declare no competing financial interest.

ACKNOWLEDGMENTS

The authors acknowledge the National Science Foundation (CHE-1800110) for support. X-ray diffraction experiments were performed using a crystal diffractometer acquired through an NSF-MRI award (CHE-1229400) in the X-ray laboratory supervised by Dr. Victor G. Young, Jr.

REFERENCES

- (1) Wang, J.; Sánchez-Roselló, M.; Aceña, J. L.; del Pozo, C.; Sorochinsky, A. E.; Fustero, S.; Soloshonok, V. A.; Liu, H. Fluorine in Pharmaceutical Industry: Fluorine-Containing Drugs Introduced to the Market in the Last Decade (2001–2011). *Chem. Rev.* **2014**, *114*, 2432.
- (2) Li, P.; Oyang, X.; Xie, X.; Guo, Y.; Li, Z.; Xi, J.; Zhu, D.; Ma, X.; Liu, B.; Li, J.; Xiao, Z. Perfluorooctanoic acid and perfluorooctane sulfonate co-exposure induced changes of metabolites and defense pathways in lettuce leaves. *Environ. Pollut.* **2020**, 256, 113512.
- (3) Chen, H.; Reinhard, M.; Yin, T.; Nguyen, T. V.; Tran, N. H.; Yew-Hoong Gin, K. Multi-compartment distribution of perfluoroalkyl and polyfluoroalkyl substances (PFASs) in an urban catchment system. *Water Res.* **2019**, *154*, 227.
- (4) Cao, X.; Wang, C.; Lu, Y.; Zhang, M.; Khan, K.; Song, S.; Wang, P.; Wang, C. Occurrence, sources and health risk of polyfluoroalkyl substances (PFASs) in soil, water and sediment from a drinking water source area. *Ecotoxicol. Environ. Saf.* 2019, 174, 208.
- (5) Stanifer, J. W.; Stapleton, H. M.; Souma, T.; Wittmer, A.; Zhao, X.; Boulware, L. E. Perfluorinated Chemicals as Emerging Environmental Threats to Kidney Health. *Clin. J. Am. Soc. Nephrol.* **2018**, *13*, 1479.
- (6) Luo, Y.-R. Comprehensive Handbook of Chemical Bond Energies, 1st ed.; CRC Press: Boca Raton, FL, 2007; p 211.
- (7) Kraft, B. M.; Lachicotte, R. J.; Jones, W. D. Aliphatic Carbon-Fluorine Bond Activation Using $(C_5Me_5)_2ZrH_2$. J. Am. Chem. Soc. **2000**, 122, 8559.
- (8) Kiplinger, J. L.; Richmond, T. G. Group IV Metallocene-Mediated Synthesis of Fluoroaromatics via Selective Defluorination of Saturated Perfluorocarbons. *J. Am. Chem. Soc.* **1996**, *118*, 1805.
- (9) Sabater, S.; Mata, J. A.; Peris, E. Hydrodefluorination of carbon–fluorine bonds by the synergistic action of a ruthenium–palladium catalyst. *Nat. Commun.* **2013**, *4*, 2553.
- (10) Senaweera, S. M.; Singh, A.; Weaver, J. D. Photocatalytic Hydrodefluorination: Facile Access to Partially Fluorinated Aromatics. *J. Am. Chem. Soc.* **2014**, *136*, 3002.
- (11) Árévalo, A.; Tlahuext-Aca, A.; Flores-Alamo, M.; García, J. J. On the Catalytic Hydrodefluorination of Fluoroaromatics Using

- Nickel Complexes: The True Role of the Phosphine. J. Am. Chem. Soc. 2014, 136, 4634.
- (12) Li, J.; Zheng, T.; Sun, H.; Li, X. Selectively catalytic hydrodefluorination of perfluoroarenes by Co(PMe₃)₄ with sodium formate as reducing agent and mechanism study. *Dalton Trans.* **2013**, 42, 13048.
- (13) Vela, J.; Smith, J. M.; Yu, Y.; Ketterer, N. A.; Flaschenriem, C. J.; Lachicotte, R. J.; Holland, P. L. Synthesis and Reactivity of Low-Coordinate Iron(II) Fluoride Complexes and Their Use in the Catalytic Hydrodefluorination of Fluorocarbons. *J. Am. Chem. Soc.* **2005**, *127*, 7857.
- (14) Hein, N. M.; Pick, F. S.; Fryzuk, M. D. Synthesis and Reactivity of a Low-Coordinate Iron(II) Hydride Complex: Applications in Catalytic Hydrodefluorination. *Inorg. Chem.* **2017**, *56*, 14513.
- (15) Schwartsburd, L.; Mahon, M. F.; Poulten, R. C.; Warren, M. R.; Whittlesey, M. K. Mechanistic Studies of the Rhodium NHC Catalyzed Hydrodefluorination of Polyfluorotoluenes. *Organometallics* **2014**, *33*, 6165.
- (16) Edelbach, B. L.; Jones, W. D. Mechanism of Carbon-Fluorine Bond Activation by $(C_5Me_5)Rh(PMe_3)H_2$. J. Am. Chem. Soc. 1997, 119. 7734.
- (17) Aizenberg, M.; Milstein, D. Homogeneous rhodium complexcatalyzed hydrogenolysis of C-F bonds. J. Am. Chem. Soc. 1995, 117, 8674
- (18) Aizenberg, M.; Milstein, D. Catalytic Activation of Carbon-Fluorine Bonds by a Soluble Transition Metal Complex. *Science* **1994**, 265, 359.
- (19) Macgregor, S. A.; McKay, D.; Panetier, J. A.; Whittlesey, M. K. Computational study of the hydrodefluorination of fluoroarenes at $[Ru(NHC)(PR_3)_2(CO)(H)_2]$: predicted scope and regioselectivities. *Dalton Trans.* **2013**, 42, 7386.
- (20) Xiao, J.; Wu, J.; Zhao, W.; Cao, S. NiCl₂(PCy₃)₂-catalyzed hydrodefluorination of fluoroarenes with LiAl(O-*t*-Bu)₃H. *J. Fluorine Chem.* **2013**, *146*, *76*.
- (21) Weidauer, M.; Irran, E.; Someya, C. I.; Haberberger, M.; Enthaler, S. Nickel-catalyzed hydrodehalogenation of aryl halides. *J. Organomet. Chem.* **2013**, 729, 53.
- (22) Gianetti, T. L.; Bergman, R. G.; Arnold, J. Carbon-fluorine bond cleavage in fluoroarenes via a niobium(III) imido complex: from stoichiometric to catalytic hydrodefluorination. *Chem. Sci.* **2014**, *5*, 2517
- (23) Pike, S. D.; Crimmin, M. R.; Chaplin, A. B. Organometallic chemistry using partially fluorinated benzenes. *Chem. Commun.* **2017**, 52, 3615
- (24) Beaumier, E. P.; Pearce, A. J.; See, X. Y.; Tonks, I. A. Modern applications of low-valent early transition metals in synthesis and catalysis. *Nat. Rev. Chem.* **2019**, *3*, 15.
- (25) Fout, A. R.; Scott, J.; Miller, D. L.; Bailey, B. C.; Pink, M.; Mindiola, D. J. Dehydrofluorination of Hydrofluorocarbons by Titanium Alkylidynes via Sequential C-H/C-F Bond Activation Reactions. A Synthetic, Structural, and Mechanistic Study of 1,2-CH Bond Addition and β -Fluoride Elimination. *Organometallics* **2009**, 28, 331.
- (26) Bosque, R.; Clot, E.; Fantacci, S.; Maseras, F.; Eisenstein, O.; Perutz, R. N.; Renkema, K. B.; Caulton, K. G. Inertness of the Aryl-F Bond toward Oxidative Addition to Osmium and Rhodium Complexes: Thermodynamic or Kinetic Origin? *J. Am. Chem. Soc.* 1998, 120, 12634.
- (27) Eisenstein, O.; Milani, J.; Perutz, R. N. Selectivity of C–H Activation and Competition between C–H and C–F Bond Activation at Fluorocarbons. *Chem. Rev.* **2017**, *117*, 8710.
- (28) Whittlesey, M. K.; Peris, E. Catalytic Hydrodefluorination with Late Transition Metal Complexes. ACS Catal. 2014, 4, 3152.
- (29) Braun, T.; Wehmeier, F. C-F Bond Activation of Highly Fluorinated Molecules at Rhodium: From Model Reactions to Catalysis. Eur. J. Inorg. Chem. 2011, 2011, 613.
- (30) Baumgartner, R.; Stieger, G. K.; McNeill, K. Complete Hydrodehalogenation of Polyfluorinated and Other Polyhalogenated

- Benzenes under Mild Catalytic Conditions. *Environ. Sci. Technol.* 2013, 47, 6545.
- (31) Young, R. J.; Grushin, V. V. Catalytic C-F Bond Activation of Nonactivated Monofluoroarenes. *Organometallics* **1999**, *18*, 294.
- (32) Gair, J. J.; Grey, R. L.; Giroux, S.; Brodney, M. A. Palladium Catalyzed Hydrodefluorination of Fluoro-(hetero)arenes. *Org. Lett.* **2019**, *21*, 2482.
- (33) Mai, V. H.; Nikonov, G. I. Hydrodefluorination of Fluoroaromatics by Isopropyl Alcohol Catalyzed by a Ruthenium NHC Complex. An Unusual Role of the Carbene Ligand. *ACS Catal.* **2016**, *6*, 7956.
- (34) Cammarota, R. C.; Lu, C. C. Tuning Nickel with Lewis Acidic Group 13 Metalloligands for Catalytic Olefin Hydrogenation. *J. Am. Chem. Soc.* **2015**, *137*, 12486.
- (35) You, D.; Gabbaï, F. P. Tunable σ -Accepting, Z-Type Ligands for Organometallic Catalysis. *Trends Chem.* **2019**, *1*, 485.
- (36) Parkin, G. A Simple Description of the Bonding in Transition-Metal Borane Complexes. *Organometallics* **2006**, 25, 4744.
- (37) Bouhadir, G.; Bourissou, D. Complexes of ambiphilic ligands: reactivity and catalytic applications. *Chem. Soc. Rev.* **2016**, *45*, 1065.
- (38) Kameo, H.; Hashimoto, Y.; Nakazawa, H. Synthesis of Rhodaboratranes Bearing Phosphine-Tethered Boranes: Evaluation of the Metal—Boron Interaction. *Organometallics* **2012**, *31*, 3155.
- (39) Moore, J. T.; Smith, N. E.; Lu, C. C. Structure and dynamic NMR behavior of rhodium complexes supported by Lewis acidic group 13 metallatranes. *Dalton Trans.* **2017**, *46*, 5689.
- (40) Sircoglou, M.; Bontemps, S.; Bouhadir, G.; Saffon, N.; Miqueu, K.; Gu, W.; Mercy, M.; Chen, C.-H.; Foxman, B. M.; Maron, L.; Ozerov, O. V.; Bourissou, D. Group 10 and 11 Metal Boratranes (Ni, Pd, Pt, CuCl, AgCl, AuCl, and Au⁺) Derived from a Triphosphine-Borane. *J. Am. Chem. Soc.* **2008**, *130*, 16729.
- (41) Kuriakose, N.; Zheng, J.-J.; Saito, T.; Hara, N.; Nakao, Y.; Sakaki, S. Characterization of Rh–Al Bond in Rh(PAlP) (PAlP = Pincer-type Diphosphino-Aluminyl Ligand) in Comparison with $Rh(L)(PMe_3)_2$ (L = AlMe₂, Al(NMe₂)₂, BR₂, SiR₃, CH₃, Cl, or OCH₃): Theoretical Insight. *Inorg. Chem.* **2019**, *58*, 4894.
- (42) Hara, N.; Saito, T.; Semba, K.; Kuriakose, N.; Zheng, H.; Sakaki, S.; Nakao, Y. Rhodium Complexes Bearing PAIP Pincer Ligands. J. Am. Chem. Soc. 2018, 140, 7070.
- (43) Shih, W.-C.; Gu, W.; MacInnis, M. C.; Timpa, S. D.; Bhuvanesh, N.; Zhou, J.; Ozerov, O. V. Facile Insertion of Rh and Ir into a Boron—Phenyl Bond, Leading to Boryl/Bis(phosphine) PBP Pincer Complexes. *J. Am. Chem. Soc.* **2016**, *138*, 2086.
- (44) Brewster, T. P.; Nguyen, T. H.; Li, Z.; Eckenhoff, W. T.; Schley, N. D.; DeYonker, N. J. Synthesis and Characterization of Heterobimetallic Iridium—Aluminum and Rhodium—Aluminum Complexes. *Inorg. Chem.* **2018**, *57*, 1148.
- (45) Cordero, B.; Gomez, V.; Platero-Prats, A. E.; Reves, M.; Echeverria, J.; Cremades, E.; Barragan, F.; Alvarez, S. Covalent radii revisited. *Dalton Trans.* **2008**, 2832.
- (46) Li, B. Z.; Qian, Y. Y.; Liu, J.; Chan, K. S. Consecutive Aromatic Carbon–Fluorine Bond and Carbon–Hydrogen Bond Activations by Iridium Porphyrins. *Organometallics* **2014**, *33*, 7059.
- (47) Peterson, T. H.; Golden, J. T.; Bergman, R. G. Deprotonation of the Transition Metal Hydride (η^5 -C₅Me₅)(PMe₃)IrH₂. Synthesis and Chemistry of the Strongly Basic Lithium Iridate (η^5 -C₅Me₅)-(PMe₃)Ir(H)(Li). Organometallics **1999**, 18, 2005.
- (48) Nakai, H.; Jeong, K.; Matsumoto, T.; Ogo, S. Catalytic C–F Bond Hydrogenolysis of Fluoroaromatics by $[(\eta^5-C_5Me_5)RhI(2,2'-bipyridine)]$. *Organometallics* **2014**, *33*, 4349.
- (49) Braun, T.; Noveski, D.; Ahijado, M.; Wehmeier, F. Hydrodefluorination of pentafluoropyridine at rhodium using dihydrogen: detection of unusual rhodium hydrido complexes. *Dalton Trans.* **2007**, 3820
- (50) Exner, J. H.; Steiner, E. C. Solvation and ion pairing of alkalimetal alkoxides in dimethyl sulfoxide. Conductometric studies. *J. Am. Chem. Soc.* **1974**, *96*, 1782.

- (51) Puri, M.; Gatard, S.; Smith, D. A.; Ozerov, O. V. Competition Studies of Oxidative Addition of Aryl Halides to the (PNP)Rh Fragment. *Organometallics* **2011**, *30*, 2472.
- (52) Gatard, S.; Guo, C.; Foxman, B. M.; Ozerov, O. V. Thioether, Dinitrogen, and Olefin Complexes of (PNP)Rh: Kinetics and Thermodynamics of Exchange and Oxidative Addition Reactions. *Organometallics* **2007**, *26*, 6066.
- (53) Kameo, H.; Yamamoto, J.; Asada, A.; Nakazawa, H.; Matsuzaka, H.; Bourissou, D. Palladium—Borane Cooperation: Evidence for an Anionic Pathway and Its Application to Catalytic Hydro-/Deutero-dechlorination. *Angew. Chem., Int. Ed.* **2019**, *58*, 18783.
- (54) Obligacion, J. V.; Bezdek, M. J.; Chirik, P. J. C(sp²)–H Borylation of Fluorinated Arenes Using an Air-Stable Cobalt Precatalyst: Electronically Enhanced Site Selectivity Enables Synthetic Opportunities. *J. Am. Chem. Soc.* **2017**, *139*, 2825.
- (55) Selmeczy, A. D.; Jones, W. D.; Partridge, M. G.; Perutz, R. N. Selectivity in the activation of fluorinated aromatic hydrocarbons by rhodium complexes $[(C_5H_5)Rh(PMe_3)]$ and $[(C_5Me_5)Rh(PMe_3)]$. Organometallics **1994**, 13, 522.
- (56) Vollmer, M. V.; Ye, J.; Linehan, J. C.; Graziano, B. J.; Preston, A.; Wiedner, E. S.; Lu, C. C. Cobalt-Group 13 Complexes Catalyze CO₂ Hydrogenation via a Co(-I)/Co(I) Redox Cycle. *ACS Catal.* **2020**, *10*, 2459.
- (57) Findlater, M.; Schultz, K. M.; Bernskoetter, W. H.; Cartwright-Sykes, A.; Heinekey, D. M.; Brookhart, M. Dihydrogen Complexes of Iridium and Rhodium. *Inorg. Chem.* **2012**, *51*, 4672.
- (58) Douglas, T. M.; Brayshaw, S. K.; Dallanegra, R.; Kociok-Köhn, G.; Macgregor, S. A.; Moxham, G. L.; Weller, A. S.; Wondimagegn, T.; Vadivelu, P. Intramolecular Alkyl Phosphine Dehydrogenation in Cationic Rhodium Complexes of Tris(cyclopentylphosphine). *Chem. Eur. J.* 2008, *14*, 1004.
- (59) Oldham, W. J.; Hinkle, A. S.; Heinekey, D. M. Synthesis and Characterization of Hydrotris(pyrazolyl)borate Dihydrogen/Hydride Complexes of Rhodium and Iridium. *J. Am. Chem. Soc.* **1997**, *119*, 11028.
- (60) Butler, S. J. Quantitative determination of fluoride in pure water using luminescent europium complexes. *Chem. Commun.* **2015**, *51*, 10879.
- (61) Zhou, J.; Kuntze-Fechner, M. W.; Bertermann, R.; Paul, U. S. D.; Berthel, J. H. J.; Friedrich, A.; Du, Z.; Marder, T. B.; Radius, U. Preparing (Multi)Fluoroarenes as Building Blocks for Synthesis: Nickel-Catalyzed Borylation of Polyfluoroarenes via C–F Bond Cleavage. J. Am. Chem. Soc. 2016, 138, 5250.
- (62) Liu, X.-W.; Echavarren, J.; Zarate, C.; Martin, R. Ni-Catalyzed Borylation of Aryl Fluorides via C-F Cleavage. *J. Am. Chem. Soc.* **2015**, 137, 12470.
- (63) Lindup, R. J.; Marder, T. B.; Perutz, R. N.; Whitwood, A. C. Sequential C–F activation and borylation of fluoropyridines via intermediate Rh(I) fluoropyridyl complexes: a multinuclear NMR investigation. *Chem. Commun.* **2007**, 3664.
- (64) Lim, S.; Song, D.; Jeon, S.; Kim, Y.; Kim, H.; Lee, S.; Cho, H.; Lee, B. C.; Kim, S. E.; Kim, K.; Lee, E. Cobalt-Catalyzed C-F Bond Borylation of Aryl Fluorides. *Org. Lett.* **2018**, *20*, 7249.
- (65) Niwa, T.; Ochiai, H.; Hosoya, T. Copper-Catalyzed ipso-Borylation of Fluoroarenes. ACS Catal. 2017, 7, 4535.
- (66) Niwa, T.; Ochiai, H.; Watanabe, Y.; Hosoya, T. Ni/Cu-Catalyzed Defluoroborylation of Fluoroarenes for Diverse C-F Bond Functionalizations. *J. Am. Chem. Soc.* **2015**, *137*, 14313.
- (67) Kalläne, S. I.; Teltewskoi, M.; Braun, T.; Braun, B. C-H and C-F Bond Activations at a Rhodium(I) Boryl Complex: Reaction Steps for the Catalytic Borylation of Fluorinated Aromatics. Organometallics 2015, 34, 1156.
- (68) Teltewskoi, M.; Panetier, J. A.; Macgregor, S. A.; Braun, T. A Highly Reactive Rhodium(I)—Boryl Complex as a Useful Tool for C—H Bond Activation and Catalytic C—F Bond Borylation. *Angew. Chem., Int. Ed.* **2010**, *49*, 3947.
- (69) Fujii, I.; Semba, K.; Li, Q.-Z.; Sakaki, S.; Nakao, Y. Magnesiation of Aryl Fluorides Catalyzed by a Rhodium—Aluminum Complex. J. Am. Chem. Soc. 2020 ASAP. DOI: 10.1021/jacs.0c04905.